System level heat pump model for investigations into thermal management of electric vehicles at low temperatures.

James Jeffs[1] Dr. Andrew McGordon[1] Alessandro Picarelli[2] Dr. Simon Robinson[3] Dr. W. Dhammika Widanage[1]

[1]WMG, University of Warwick, United Kingdom, j.jeffs@warwick.ac.uk
[2]Claytex ltd., United Kingdom, alessandro.picarelli@claytex.com@company
[3]Jaguar Land Rover, United Kingdom, srobin43@jaguarlandrover.com

Abstract

One of the challenges concerning electric vehicles is their performance in cold climates. As the temperature drops below 10°C battery capacity begins to reduce and heating demand starts to claim a larger proportion of total vehicle energy expenditure. Although efficient, electric vehicles waste heat through a few components, resulting in opportunity to harvest waste heat through a heat pump. With multiple options for harvesting heat and the option to heat the battery, a model and architecture has been developed to give flexibility in a wide range of thermal management scenarios. This paper explores the details of the model and presents two example cases of interest to demonstrate the model's applicability.

Keywords: Electric vehicle, thermal management, heat pump

1 Introduction

With electric vehicles beginning to take a larger market share of new vehicle sales, one common concern of electric vehicle drivers is the choice they may have to make at low temperature between heating and range (Allen, 2013; Bullis, 2013). Operation of electric vehicles below 10°C is hindered by the effect of low temperatures on battery capacity and the increased electrical consumption caused by cabin heating (Meyer et al., 2012). The combined effect of decreased battery performance and increased heating demand gives a range loss of up to 60% at −20°C compared to 20°C. Heat pumps are slowly being introduced as a solution to this problem; however the flexibility of heat pumps creates an opportunity for new, innovative and complex thermal management solutions, with many operational modes available for consideration and exploration (Jeffs et al., 2018).

1.1 Battery performance at low temperatures

Many investigations have been carried out into the performance of Lithium ion cells at low temperatures. The three areas which are cause for concern are ageing, power and capacity. The consensus on ageing of cells at low temperatures is that charging causes the formation of metallic lithium on the cathode, a process known as lithium plating. Lithium plating is associated with fast charging of a cell (over 0.5C, where 1C is the the current required to charge the cell in one hour) and so can be avoided by charging slowly and reducing the power harvested through regenerative braking. Power reduction has also been a concern when operating cells at low temperatures. Rui (Rui et al., 2011), Zheng (Zheng et al., 2016) and Jaguemont (Jaguemont et al., 2016) concluded that the primary cause of power capability reduction was due to an increase in charge transfer resistance. However, it has also been shown that for a typical pack sizing, a 70% reduction in power can be sustained while the vehicle is still able to complete usual drive cycles (UDDS, HWFET, US06) (Saxena et al., 2015). Reflecting on this literature, precautions are built into the model to take account of power reduction and increased ageing.

The biggest concern regarding electric vehicle operation at low temperatures is the reduction in range associated with reduced capacity. Much research has been published reporting cell capacity as a function of temperature and some examples are summarised in Figure 1 which displays the work of Nagasubramanian (Nagasubramanian, 2001), Zhang (Zhang et al., 2003), Ji (Ji et al., 2013), Jaguemont (Jaguemont et al., 2014), Dow Kokam (Dow, 2010) (manufacturer) and Panasonic (Pan, 2012) (manufacturer). The general consensus reached through this selection of work is that cell capacity decreases by approximately $20-40\%$ at $-20°C$ and by as much as 70% at $-40°C$.

1.2 Cabin Heating

Cabin heating is the greatest non-powertrain consumer of energy on a vehicle at low temperatures (Lindgren and Lund, 2016; Broglia et al., 2012). In early production electric vehicles such as the first generation Nissan Leaf, the cabin heat was provided by a positive thermal coefficient (PTC) heater. PTC heaters are close to 100% efficient, but generate all of their heat using electrical energy from the battery. Due to the high demand of cabin heating, typically 4-7kW, this has a significant impact on the vehicle's range. Meyer *et al.* (Meyer et al., 2012) investigated the split between the impact of cabin heating and low temperature battery effects; performing tests with heating on

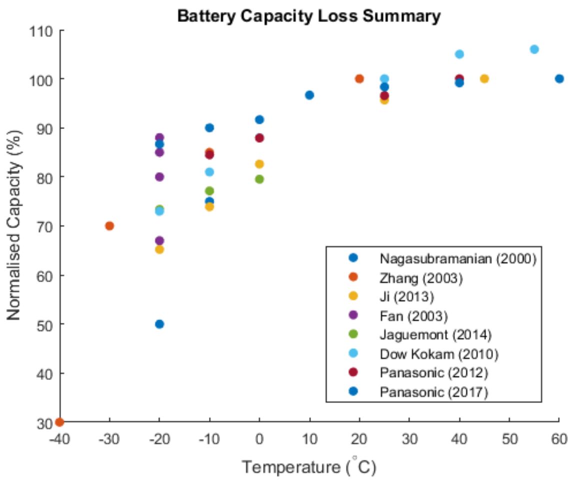

Figure 1. A summary of the capacity loss a function of temperature as reported by the following sources; Nagasubramanian (Nagasubramanian, 2001), Zhang (Zhang et al., 2003), Ji (Ji et al., 2013), Jaguemont (Jaguemont et al., 2014), Dow Kokam (Dow, 2010) (manufacturer) and Panasonic (Pan, 2012) (manufacturer).

full (continuously), and heating off at −7°C. During the two tests at −7°C over the LA4 drive cycle (also known as FTP-72 or the Urban Dynamometer Driving Schedule), Meyer *et al.* = found that the use of PTC heaters led to a 41% reduction in vehicle range compared to its 20°C range. In comparison, a range reduction of just 15% was found with the heating off at the same temperature, which can be attributed to the effect of low temperatures on an Li-ion battery. The combined effect of heating demand and reduced battery capacity is a 60% reduction in range at −20°C (Reyes et al., 2016).

Heat pumps are now becoming more dominant as a solution to vehicle heating, with examples found in vehicles such as; Jaguar iPace, BMW i3, Nissan Leaf (latest generation), Renault Zoe and others. The main advantage of a heat pump is that it doesn't solely generate heat, but can extract and upgrade heat; making it useful for cabin heating. This can be done at more than 100% efficiency. Examples of research in this area include Leighton *et al.* (Leighton, 2015), who demonstrated a lab bench system capable of extracting heat from ambient; upgrading it with heat from power electronics and a PTC heater, then heating the cabin and battery. In this example the power electronics, PTC heater, cabin and battery were in series in a coolant loop with the heat pump's condenser in the order stated. In 2014 Ahn *et al.* proposed a dual source heat pump which could harvest waste heat from the motor as well as ambient; this can be distinguished from Leighton's work as the motor would be located on the evaporator loop, rather than the condenser loop. Using simulation, Ahn showed that the addition of waste heat from the motor increased the maximum coefficient of performance (COP) from 3 to 3.4, but also allowed the heat pump to work more effectively at lower temperatures, where heat extraction from ambient is more difficult. In 2017 Jeffs *et al.* proposed the use of a thermal battery to further assist energy saving at low temperature. They showed that an optimally sized thermal battery would be able to effectively replace the PTC heater, which was previously needed to aid heat pump warm up. Here an average energy saving of 25.3% was made over a temperature range of −20°C to 14°C using a cruising drive cycle, while not compromising cabin warm up times (Jeffs et al., 2017). This selection of work shows the range of use cases which a heat pump may be subjected to, a point further demonstrated by Jeffs *et al.* in 2018, where 32 operational modes where identified and compared for a multiple source heat pump on an electric vehicle (Jeffs et al., 2018).

1.3 Goals for Model capability

From section 1.2 it is clear that a consensus on a thermal management architecture from low temperature perspective has not been reached. With multiple components on the vehicle wasting heat, as well as the added complexity of balancing cabin and battery heating, and the added complexity of optimally operating a heat pump in a dynamic environment, a model which allows users to flexibly reconfigure the thermal architecture of the vehicle could help guide the thermal architecture on vehicles in the future.

The model developed in this work has the objective of providing the following features.

1. The ability to dynamically connect and disconnect components from the thermal management system.
2. The ability to arbitrarily request heat flows between components (e.g. request 5kW for cabin heating), while being physically limited by sensibly sized heat exchangers.
3. Contain a control system for the heat pump which self regulates compressor speed regardless of vehicle configuration.
4. Run quickly enough to be useful for performing parameter sweeps and optimisations in suitable time frames. (PC configuration: Laptop, using i7-6600U @ 2.6GHz with 16GB RAM. Dymola version 2019 using Visual Studio 2015/Visual C++ 2015 Express Edition (14.0).)

2 Method

Here the details of the models are discussed with justifications of choices made during the development process. The top level of the vehicle is shown in Figure 2. In this figure the sub-models; heatDemandCommander, heat pump control unit HPCU, battery, Heat Pump, and Cabin model can be seen. These sub-models will be discussed in more detail in the following subsections, starting with the battery. Following the description of the model, two test

DOI 10.3384/ecp19157107

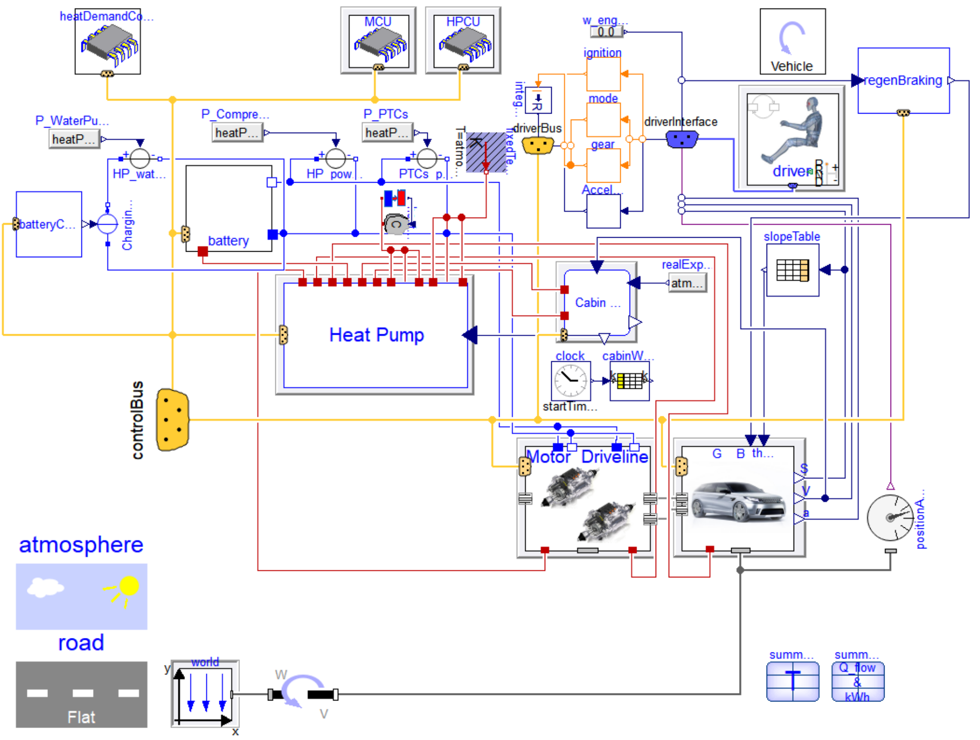

Figure 2. The top level of the model is shown.

cases are presented which demonstrate the model's versatility.

The model has been developed using Dymola based on the Modelica language. This work relies on the following libraries and providers; "Claytex VeSyMA-Powertrain" and "TLK-Thermal Systems library".

2.1 Battery

The battery is modelled both electrically and thermally. The electric side uses a first order RC network equivalent circuit model (ECM), as seen in Figure 3. The components in this model are parameterised using look up tables which are a function of component temperature, as measured using the thermal model, and the cell's state of charge (SOC). The resistor and open circuit voltage (OCV) values are scaled by the number of cells in series to produce an RC circuit which represents one string of the pack. This data was generated specifically for Xalt 40Ah cells by Yashraj Tripathy in (Tripathy et al., 2018). This type of battery model is typically seen in literature (Jaguemont et al., 2016; Ruan et al., 2014) when modelling pack size batteries for vehicle application. In this application the vehicle was configured in a 2p108s (2 parallel strings of 108 cells in series) arrangement giving a pack size of approximately 30kWh; although altering the pack size for different operations is possible. This can be achieved by reducing the number of cells in series by adjusting nS_cell, seen in the top left of Figure 3, this will also automatically adjust the sizing of thermal mass in the thermal model. Alternatively, individual strings may be deleted or duplicated, changing the number of cells in series, this would require the re-parametrisation of the thermal and state of charge models accordingly.

Since the parameters of the RC network are dependent on temperature, a thermal model was created to estimate the bulk temperature of the pack. Figure 3 shows that the ohmic losses from the resistors in the circuit are calculated and exported from the sub-model as Total waste power. The sum of these losses from each string in parallel is used as the heat generation through losses in the thermal model. The thermal model can be seen in Figure 4. In this model the heatCapacitor seen in the centre represents the bulk of the battery and its temperature is used as the battery temperature. It has three modes of heat exchange; input heat from waste heat generation in the cells, interaction with the thermal management system, and thermal losses to ambient. The latter heat exchange is modelled using the flat plate parallel flow equation (Bergman et al., 2011), given in Equation 1,

$$\bar{h} = (0.037Re^{4/5} - 871)Pr^{1/3}\frac{k}{L} \quad (1)$$

where k, Re and Pr are the thermal conductivity, Reynolds number and Prandtl number of the convection fluid. The Reynolds number and Prandtl number are defined in Equations 2 and 3. L is the length of the surface over which the fluid is flowing, here $4m$ is used as an approximation of the length of the underside of the vehicle.

$$Re = \frac{\rho v L}{\mu} \quad (2)$$

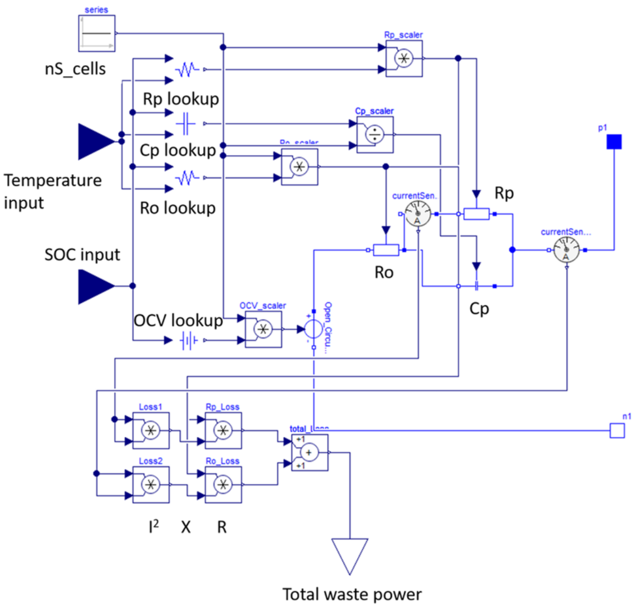

Figure 3. Electric first order RC model for the battery, scaled by number of cells in series using parameter nS_cells, seen in the top right.

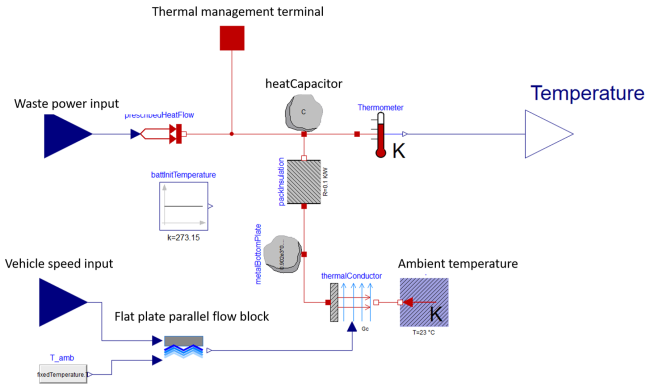

Figure 4. Thermal model of the battery with heat exchanges between ambient through a resistor to an exterior metal plate, and to the thermal management system through heat port seen at the top of the figure.

$$Pr = \frac{C_p \mu}{k} \tag{3}$$

In Equations 2 and 3 ρ, v, μ and C_p are density, velocity, dynamic viscosity and specific heat capacity of convective fluid, in this case air. The final heat flow to ambient is then given by

$$Q_{ambient} = \bar{G}(T_{plate} - T_{ambient}) \tag{4}$$

or

$$Q_{ambient} = \bar{h} \times W \times D \times L(T_{plate} - T_{ambient}). \tag{5}$$

It should be noted from literature that the capacity of a battery is dependent of its temperature; in research concerning the operation of electric vehicles in low temperatures this should be accounted for. The state of charge model is used to estimate the state of charge of the battery through the drive cycle as a function of temperature. To achieve this, the state of charge model has an additional lookup table which contains information about the percentage of capacity available as a function of temperature. This is then used to scale the Coulomb counting equation by the factor C_{eff} seen in Equation 6. Other examples of this adjustment to Coulomb counting can be seen in (Tripathy et al., 2018) and (Barai et al., 2016).

$$SOC(t) = SOC_{init} - \frac{1}{C_{eff}} \int_0^t I(t)dt \tag{6}$$

2.2 Cabin

The cabin has a target temperature of 22°C which can be used to assess the thermal comfort achieved when using the heat pump. The cabin model can be seen in Figure 5. An infinite air source with ambient temperature is taken into the cabin and heated in the eAC component, seen in Figure 5. The heated air is then pumped into the cabin, where a single air volume and heat capacitance are used to measure the cabin temperature. This heat capacitor has four modes of loosing heat; convection to ambient through panels, thermal exchange with soft furnishings, thermal exchange with hard furnishings, and cabin air exhaust. The convection to ambient through the exterior surfaces is modelled using a variable thermal conductance with dependency on vehicle speed. The model uses two heat capacitances for air to hard furnishings (such as dashboard panels, glass etc.) and soft furnishings (such as the seats, carpet etc.), with thermal resistances between the air and these components. Finally there are two volumes representing the air in the cabin; one large and one small. The larger air volume represents the majority of the cabin where the target temperature is imposed. The smaller air volume is used to harvest cabin exhaust waste heat, here up to 30% of the heat can be extracted and used in the heat pump. This amount reflects the claims made by BMW in (Suck and Spengler, 2014).

2.3 Heat Pump

The heat pump has the flexibility to dynamically connect to, and disconnect from, components around the vehicle. There are two places in the heat pump where these connections are controlled. In Figure 6 there is a row of thermal switches at the top of the model, this is the first point of control regarding component connections. Inside these switches there is a thermal conductor which is either set to 0 to thermally isolate the component from the heat pump, or controlled by a PID controller to achieve the desired heat exchange. The desired heat flow is set in the heatDe-

DOI 10.3384/ecp19157107

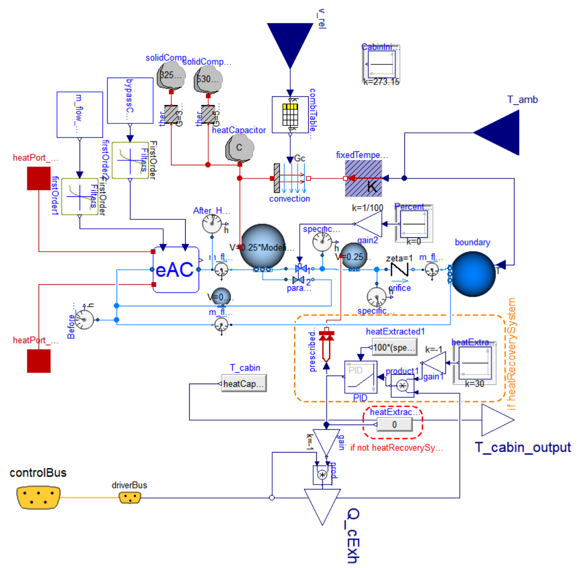

Figure 5. Cabin model

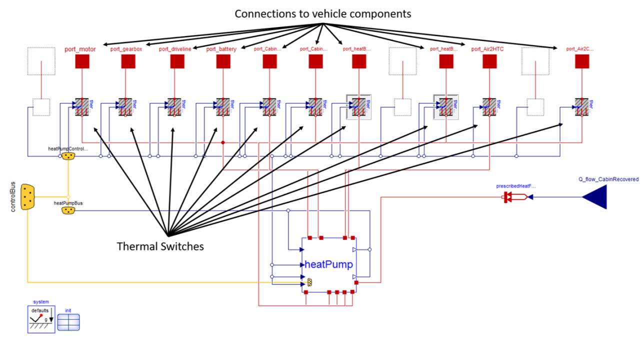

Figure 6. The uppermost level of the heat pump where thermal connections across the vehicle are made and controlled. In the centre is the middle layer of the heat pump which contains the physical models of the coolant and refrigeration circuits.

mandCommander and will be discussed further in section 2.5. This layer acts to control the thermal connection between the heat exchangers in the middle level of the heat pump model and the vehicle components. This is important as it allows for arbitrary heat demands to be requested, which might then be used to guide heat exchanger sizing or coolant control to maintain an optimal temperature in a component. The second point of control for component connections is in the coolant circuits labelled high temperature circuit (HTC) and chiller circuit, found in the middle level of the heat pump, seen in Figure 7.

The middle level of the heat pump model is used to house, pump coolant between, and direct heat flows to, the 3 main models of the heat pump. These are the HTC, chiller circuit and refrigeration loop. Inputs to this level include coolant mass flow rate (which is then controlled by a pump and PID), compressor power demand which is passed onto the refrigerant model, and cabin temperature which is used to shut off the PTC heater in the HTC. The coolant circuits themselves contain heat exchangers

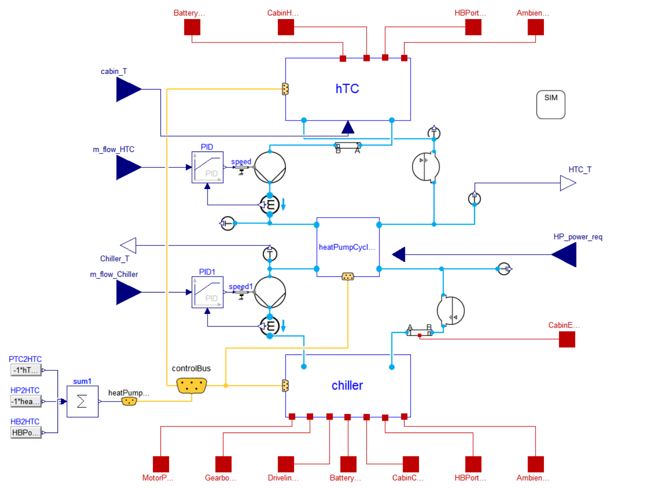

Figure 7. The middle level of the model contains the coolant circuits and the refrigeration loop and is used to control coolant flow between them.

which have been sized using examples and estimates taken from components found on existing vehicles. This level also sees the input of heat recuperated from cabin exhaust, which is used to increase the temperature of the chiller loop.

The coolant circuits, HTC and chiller are shown in Figures 8 and 9 respectively. They have operating temperatures of 90°C and −10°C respectively. In Figure 8 the thermal battery and PTC heater are in series before the coolant reaches the cabin, battery and ambient which are in parallel. It can also be seen that all components with the exception of the PTC heater have a bypass option; this is the second control point for component connections which can be used to thermally isolate a component from the system. This arrangement was chosen so that thermal battery could be used to increase the coolant temperature from the condenser output and under certain conditions negate the need for the PTC heater, which is set to turn off if the coolant temperature exceeds 85°C. The hot coolant is then split between the battery and the cabin, giving the user flexibility in selecting how much heat to send to each component; either by using the heatDemandCommander, setting different bypass amounts for each component, or adjusting the heat exchanger sizing. Here it should be mentioned that the PTC heater is controlled by a PID with the objective of getting the cabin to its set point, unless shut off by excessive coolant temperature.

The chiller circuit is arranged in a similar way to the HTC, as seen in Figure 9, with the components capable of contributing heat to the system set in parallel. These heat exchangers allow heat to be extracted from; the motor and inverter (as one unit), the gearbox and driveline (which will be treated as one component and referred to as transmission), the battery, the thermal battery, and ambient. The chiller circuit also uses bypasses to thermally isolate components from the heat pump. The bypass valves are set to values 0.99 for open and 10^{-8} for closed, to

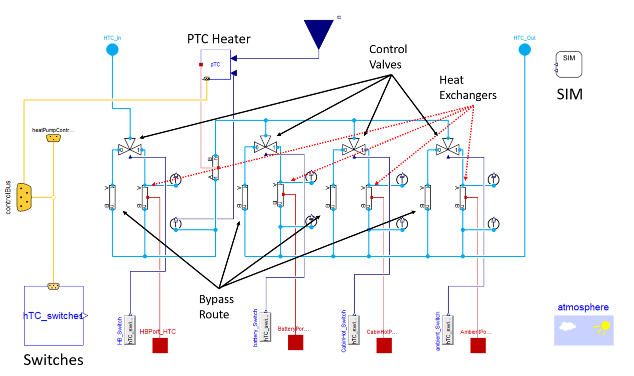

Figure 8. The coolant loop used for high temperature components, i.e. cabin and battery heating, PTC input, heat battery input, and rejecting heat to ambient for air conditioning operation.

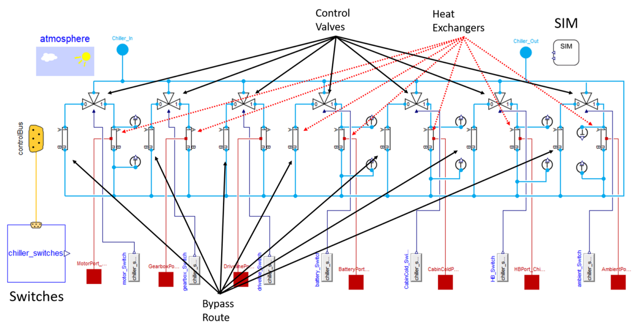

Figure 9. The chiller circuit is used for thermal exchange and extraction, i.e. extracting from the motor and inverter, the gearbox and driveline, ambient, heat battery. There is also the capability to cool the cabin and electric battery if needed.

prevent errors and problems encountered with zero flow. These valves are controlled by the switch blocks in the bottom left of Figures 8 and 9, which is connected to the controlBus and is controlled in the HPCU.

The bottom level of the heat pump contains the physical model of the refrigerant circuit. In this example R134a is used, but the refrigerant circuit may be quickly reconfigured by selecting a different refrigerant in the SIM block and changing pressure settings accordingly. The configuration of the heat circuit is typical of what may be found in literature (Leighton, 2015; Ahn et al., 2014). Since the heat exchanger has liquid coolant heat exchangers on both the condenser and evaporator sides, some care has been taken to create a control system which does not exceed the physical limits of the coolant and refrigerant set by the library. The coolant is prevented from going beyond its temperature limits using the HPCU which controls the compressor demand seen on the right of Figure 10. The refrigerant is protected from exceeding its pressure limit by the PID labelled *PID_pressureControl* seen in Figure 10, which is set to limit the pressure to 30*bar*; chosen corresponding to R134a's pressure-enthalpy diagram. Given two power demands existing at this level, the demand ac-

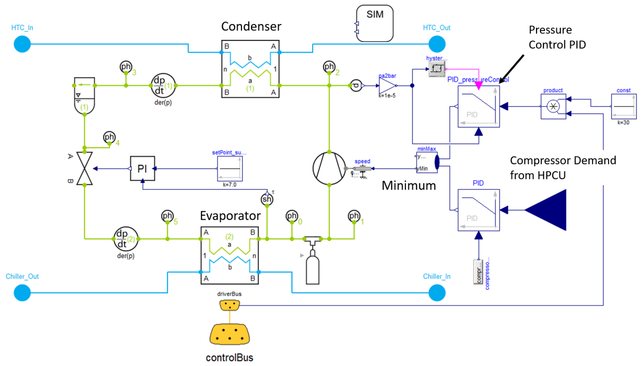

Figure 10. The refrigeration cycle is physically modelled. At this level the speed of the compressor is controlled either by the demand from the heat pump controller, or a PID which stops the system pressure getting too high.

cording to the pressure controller and the demand input from the HPCU, the minimum of these values is used to control the compressor, ensuring that neither refrigerant pressure nor coolant temperature exceed their physical limits.

2.4 Heat Pump Control Unit (HPCU)

The heat pump control unit has three purposes; firstly to set the desired coolant flow for the HTC and chiller circuits, secondly to control which components are connected to, or thermally isolated from, the heat pump, and finally to set the desired power output of the heat pump compressor. The first of these roles is done by putting a constant mass flow demand onto the control bus to be used at the heat pump middle level. For the motor and inverter (single unit), the transmission and the cabin, the thermal switching can be thought of as binary. To ensure a heat flow is created when the component is thermally active, the connection is only allowed to be made if there is a sufficient temperature difference between the component and the coolant loop. For the electric battery, thermal battery and ambient, extra rules exist for logical operation of these sources. Firstly, the electric battery is connected to the HTC (being heated) when its temperature is below 20°C; above this temperature it is thermally isolated from the heat pump. If the electric battery's temperature should rise above 30°C it is connected to the chiller (being cooled). Both these temperatures were chosen for sensible electric battery operation. The heat battery is first connected to the HTC, helping to rapidly increase the HTC temperature during the warm up phase. When it can no longer heat the HTC it is connected to the chiller, where it is fully discharged, then thermally isolated. Finally, ambient is only used as a heat source when its temperature is above -10°C, which, in a normal vehicle, would prevent frost from building up on the ambient heat exchanger, reducing its effectiveness.

The compressor controller, shown in Figure 11, has the purpose of getting the cabin and battery to temperature

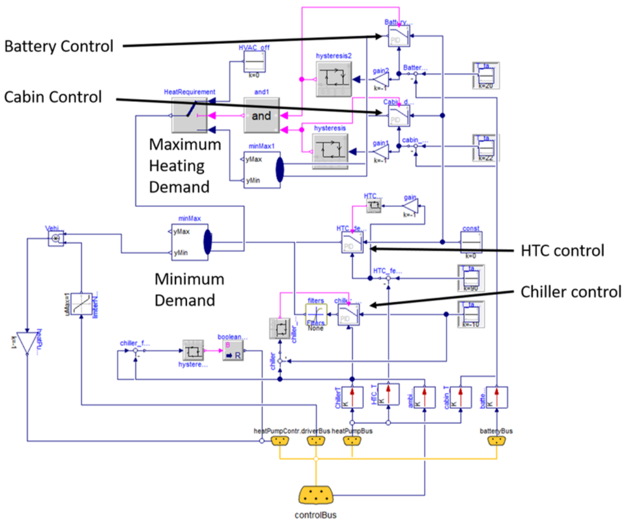

Figure 11. The compressor controller

while ensuring that the HTC and chiller don't exceed their temperature limits. PID controllers are used to create a compressor power demand according to the battery and cabin current and target temperatures, the greatest of these demands is taken to ensure there is enough heat to meet these requirements. Additionally, PID controllers are used to set a power demand needed to bring the chiller and HTC loops to their target temperatures. The minimum power request (from either the cabin and battery, the chiller and the HTC controls) is then passed to the compressor; the minimum is used so that, if a component has reached its set point, it is not pushed beyond that target by the requirements of another component. This logic prevents the battery and cabin from overheating and reduces the chance of the model failing due to the coolant breaching its temperature limits.

2.5 heatDemandCommander

This component is used to set requested heat flows for thermally active components around the vehicle. For this work constant heat flows were requested. The heat flow request is then put on the control bus to be used as the set point for PID controllers in the switches found in the heat pump, described in section 2.3.

2.6 Test cases

Here 2 unique test cases are proposed to demonstrate the flexibility of this work for testing a variety of scenarios. These test cases are:

1. Can the electric battery be used as a heat source when its temperature is above 0°C (chosen to maintain regenerative braking). To explore this case 5 scenarios will be tested and compared; 1. heating the battery (as described in section 2.4), 2. cooling the battery, 3. disconnecting the battery, 4. battery disconnected and PTC off, and 5. battery cooled with PTC off.
2. Is the transmission useful as a thermal source for the heat pump? This is tested by using ambient and transmission as heat sources, then comparing the total vehicle energy consumption and cabin temperature profile. As with the previous case, these 2 scenarios will be retested with the PTC heater off. To make a complete assessment of the transmission as a thermal contributor it will be tested in isolation, i.e. the motor will be disconnected from the heat pump leaving the transmission and ambient as the only contributors.

Both of these test cases are demonstrated at 0°C ambient temperature and using the WLTP drive cycle. While the results of these two cases will be shown in detail, the model has been used in many more scenarios.

3 Results

Here the results of the two cases will be shown and discussed.

3.1 Case 1

In this demonstration, the comparison is made between heating the battery and cooling the battery by adjusting its target temperature in the switches controller. The battery will also be disconnected from the heat pump to provide a baseline. Figure 12 shows the battery temperature through the drive cycle. Here it can be seen that the scenarios have performed as expected. When the battery is heated it quickly reaches its target temperature (20°C), at which point it is isolated from the heat pump. During this heating phase 5kW of heat flow is requested in the heatDemandCommander which is then sustained by the models controllers. Despite being disconnected from the heat pump at target temperature, the battery's temperature continues to rise due to internal resistance and self heating. Should the temperature rise above 30°C then the battery would connect to the chiller. This temperature is chosen somewhat arbitrarily, although some cooling is required to reduce ageing and mitigate against thermal runaway and other safety concerns associated with high temperature cell operation. In the second scenario it can be seen that the cooling keeps the battery temperature much lower throughout the cycle. The battery temperature rises quickly at the end of the cycle, during the high speed section; this reflects the higher losses the battery will experience through maintained lower temperatures. Finally, if the battery is not thermally managed as in the third scenario of case 1, the battery temperature is allowed to rise unaided until it is naturally limited by reduced loss and thermal loss to ambient.

Figure 13 is used to show the impact each scenario has on the cabin temperature. When the battery is heated there is less heating capacity for the cabin and hence the temperature, and therefore comfort, is reduced. When the battery is cooled there is extra thermal capacity and so the cabin is heated faster and thermal comfort is improved. However,

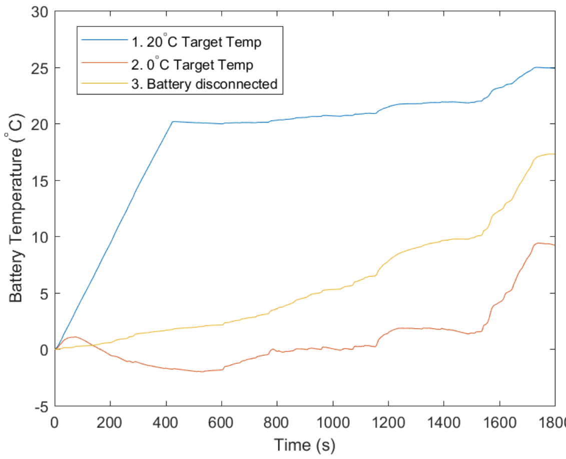

Figure 12. The battery temperature through the WLTP cycle shown for the first 3 scenarios proposed in case 1.

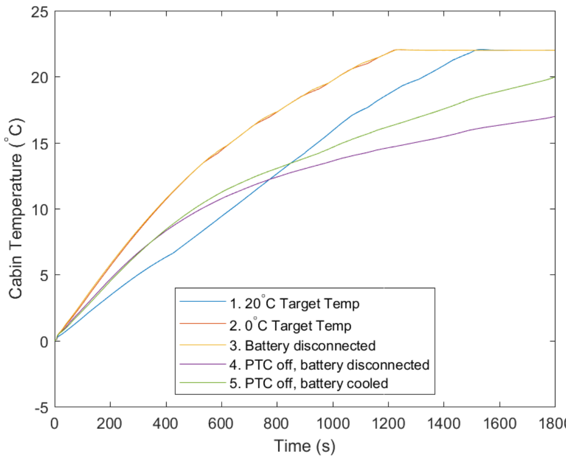

Figure 13. The cabin temperature is shown for the 3 scenarios proposed in case 1.

the extra heat that is extracted from the battery does not appear to make a significant difference to the cabin temperature compared to disconnecting the battery from the heat pump. While the extra heat from the battery should provide extra heat for the cabin, the heat pump is already saturated with heat from ambient and the motor, hence the extra heat only serves to increase the coolant temperature on the chiller. Furthermore with the additional heat from the PTC heater (on in all cases) the HTC quickly reaches temperature.

Scenarios 4 and 5 have been used to demonstrate the benefit that battery cooling can provide to cabin heating when the heat pump is not saturated with heat. Here it can be seen that the cabin temperature suffers in both scenarios where the PTC heater is off. However, the additional heat extracted from the battery now allows the cabin to heat up faster and reach a higher final temperature, compared to no heat extraction and no PTC heater.

Table 1 shows the energy consumption and the final

Table 1. The total electrical energy consumption and final SOC for the 5 scenarios proposed in case 1.

Scenario	Energy Consumed	Final SOC
1	8.08 kWh	81.1 %
2	8.24 kWh	78.5 %
3	7.68 kWh	80.8 %
4	6.45 kWh	83.9 %
5	7.68 kWh	79.6 %

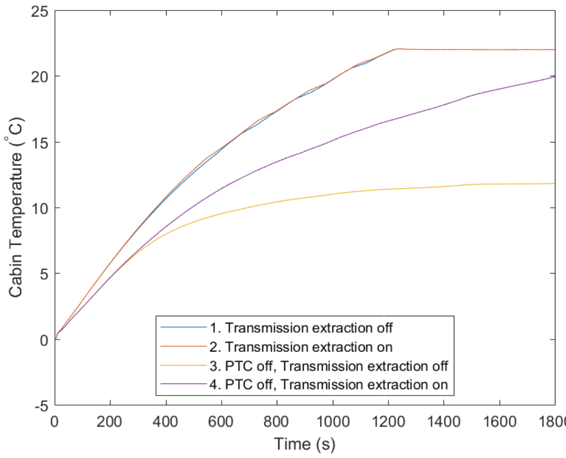

Figure 14. The cabin temperature is shown for the 4 scenarios proposed in case 2.

SOC corresponding to the 5 scenarios. Since the rate at which SOC is used is dependant on temperature, the final SOC is not directly proportional to energy consumption, but is also linked to temperature profile. Here it should be noted that scenario 1 (where the battery is heated) has a final SOC higher than scenario 2 (unheated). Operating at a higher average temperature through the cycle reduces the losses through internal resistance, increasing the terminal voltage and reducing the current required to produce the same power, hence the difference in final SOC.

With regards to point 4 of section 1.3, it took 32 minutes and 51 seconds to simulate all the scenarios required for case 1. This gives and average simulation time of 6 minutes and 34.2 seconds. Since WLTP is a 30 minute drive cycle this equates approximately 4.6 times faster than real time, meaning the simulation is adequately fast.

3.2 Case 2

Here the benefit of including the transmission as a thermal contributor to the heat pump is evaluated. This is done by comparing 4 scenarios, firstly a baseline case with ambient the thermal contributor, and secondly with the transmission as an additional contributor, then repeated with the PTC heater off.

Like in case 1 the heat pump is saturated before the transmission is introduced as a contributor; hence the heat extracted does not make a noticeable difference to the

Table 2. Total electric energy consumption for the 4 scenarios proposed in case 2

Scenario	Energy Consumed
1	7.82 kWh
2	7.68 kWh
3	6.05 kWh
4	6.72 kWh

cabin comfort, as can be seen when comparing scenarios 1 and 2 in Figure 14. As with the battery, when the PTC heater is turned off the extra heat provided to the cabin makes more of a difference, as in scenarios 3 and 4. The compromise of this extra cabin comfort is the cost of extraction and the extra load that is put on the motors due to the transmission being kept at a lower, less efficient temperature. The energy consumption for each scenario is given in Table 2.

In Table 2 it can be seen that when the PTC heater is in use (scenarios 1 & 2) the extra heat from the transmission saves energy. In other words the energy saved from reaching HTC target temperature slightly earlier, which causes the PTC heater to shut off, exceeds the costs of operating the transmission at a lower efficiency and extracting the heat. Although, since the heat pump is operating at capacity before the transmission is introduced, the cost of extraction is negligible. Considering this, in these circumstances the transmission is viable as a thermal contributor, on the condition that the engineering or implementation costs do not outweigh the potential benefits. When the PTC heater is not used, the extra costs of using the transmission do not return an energy saving and so increase total consumption. Given the extra thermal comfort provided, seen in Figure 14, this is probably a worthwhile compromise.

Again for completion, the simulation time for case 2 was 28 minutes and 40 seconds, or 7 minutes and 10 seconds per scenario, or approximately 4.2 times faster than real time. This further evidences that the model runs reliably fast, completing simulations in an adequately short amount of time.

4 Discussion

The results presented above show the variability and potential power of this model for evaluating different thermal management strategies in cold climates. One of the key questions in this area concerns the thermal management of batteries; in case 1 some scenarios are proposed and evaluated. Each scenario evaluated met the expected outcome; for example heating the battery uses more energy and reduces cabin comfort compared to disconnecting the battery from the heat pump, seen by comparing scenarios 1 and 3. It was also shown that the battery may be used as a heat source when cabin heating is not saturated, as seen in scenarios 2, 4 and 5. It is also interesting to note that the reduced battery efficiency and lower effective SOC of extracting heat from the battery means that it is not worth doing, as energy consumption and final SOC of scenario 5 are worse than scenario 3. This difference is marginal and under other circumstances (temperature, battery target temperature, battery size, ambient temperature etc.) the same may not be true. This platform gives the user the ability to easily and quickly explore these spaces.

In case 2 it was shown that the transmission is a viable contributor to the heat pump. This was demonstrated by the energy saving achieved when the PTC heater is in use, and the additional thermal comfort when it was not. Considering this further investigation into its use with a more complex system should be undertaken. While it is seen to provide a benefit on its own, in a system where cabin heat is saturated, its use may not be as valuable as seen with scenarios 1 and 2. The system proposed has the ability to further explore these scenarios and make a more complete recommendation for the use of the transmission as a thermal contributor to the heat pump.

Finally a review of the objectives that were set in section 1.3. Firstly, goal 1. is shown in the case 1, scenario 1 where the battery disconnects itself from the heat pump when it reaches its target temperature. This is an example of passive dynamic connection and disconnection, however a schedule could be implemented to directly control the connection timings. Secondly, in case 1 the model successfully sustained the requested heat flow of 5kW to the battery while it was being heated. Thirdly, in sections 2.4 and 2.3 a control system for the compressor was described which self regulates according to coolant temperatures, cabin and battery target temperatures and refrigerant pressure. This control system ensures the cabin and battery reach their target temperatures without model failing due to breach of physical limits. Fourthly and finally, in the examples shown the case 1 took 32 minutes and 51 seconds to complete, while case 2 took 28 minutes and 40 seconds to complete which are perfectly usable time frames when evaluating thermal management strategies.

5 Conclusion

The model has been demonstrated in a range of cases and scenarios. Its versatility in answering many thermal management problems has been shown and the objectives set to prove this have been met. The results from the tests proposed and evaluated are justifiable and make sense when compared to what is known about electric vehicles operating in low temperatures and the nature of heat pumps. Hence this work shows a valuable, versatile tool in exploring thermal management of complex heat pump systems on electric vehicles in low temperature climates.

Acknowledgement

This project was possible thanks to funding provided by EPSRC, funding and support from Jaguar Land Rover, and software and modelling support from Claytex Services Ltd

References

Jae Hwan Ahn, Hoon Kang, Ho Seong Lee, Hae Won Jung, Changhyun Baek, and Yongchan Kim. Heating performance characteristics of a dual source heat pump using air and waste heat in electric vehicles. *Applied Energy*, 119:1–9, 2014.

Megan Allen. http://www.fleetcarma.com/electric-car-range-in-bitter-cold/, 2013. Accessed: 29/11/2018.

Anup Barai, Kotub Uddin, WD Widanalage, Andrew McGordon, and Paul Jennings. The effect of average cycling current on total energy of lithium-ion batteries for electric vehicles. *Journal of Power Sources*, 303:81–85, 2016.

Theodore L Bergman, Frank P Incropera, David P DeWitt, and Adrienne S Lavine. *Fundamentals of heat and mass transfer*. John Wiley & Sons, 2011.

Lionel Broglia, Gabriel Autefage, and Matthieu Ponchant. Impact of passenger thermal comfort and electric devices temperature on range: a system simulation approach. *World Electric Vehicle Journal*, 5(4):1082–1089, 2012.

Kevin Bullis. https://www.technologyreview.com/s/522496/electric-vehicles-out-in-the-cold/, 2013. Accessed: 29/11/2018.

Superior Lithium Polymer Cell: Technical Data Sheet. Dow Kokam, 9 2010.

J Jaguemont, L Boulon, Y Dubé, and D Poudrier. Low temperature discharge cycle tests for a lithium ion cell. In *2014 IEEE Vehicle Power and Propulsion Conference (VPPC)*, pages 1–6. IEEE, 2014.

Joris Jaguemont, Loïc Boulon, and Yves Dubé. Characterization and modeling of a hybrid-electric-vehicle lithium-ion battery pack at low temperatures. *IEEE Transactions on Vehicular Technology*, 65(1):1–14, 2016.

J. Jeffs, A. McGordon, W. D. Widanage, S. Robinson, and A. Picarelli. Use of a thermal battery with a heat pump for low temperature electric vehicle operation. In *2017 IEEE Vehicle Power and Propulsion Conference (VPPC)*, pages 1–5, Dec 2017. doi:10.1109/VPPC.2017.8330932.

James Jeffs, Andrew McGordon, Alessandro Picarelli, Simon Robinson, Yashraj Tripathy, and Widanalage Widanage. Complex heat pump operational mode identification and comparison for use in electric vehicles. *Energies*, 11(8):2000, 2018.

Yan Ji, Yancheng Zhang, and Chao-Yang Wang. Li-ion cell operation at low temperatures. *Journal of The Electrochemical Society*, 160(4):A636–A649, 2013.

Daniel Leighton. Combined fluid loop thermal management for electric drive vehicle range improvement. *SAE International Journal of Passenger Cars-Mechanical Systems*, 8(2015-01-1709), 2015.

Juuso Lindgren and Peter D Lund. Effect of extreme temperatures on battery charging and performance of electric vehicles. *Journal of Power Sources*, 328:37–45, 2016.

Norm Meyer, Ian Whittal, Martha Christenson, and Aaron Loiselle-Lapointe. The impact of the driving cycle and climate on electrical consumption and range of fully electric passengers vehicles. In *Proceedings of EVS*, volume 26, 2012.

Ganesan Nagasubramanian. Electrical characteristics of 18650 li-ion cells at low temperatures. *Journal of applied electrochemistry*, 31(1):99–104, 2001.

Lithium Ion NCR18650. Panosonic, 2012.

J. R. M. Delos Reyes, R. V. Parsons, and R. Hoemsen. Winter happens: The effect of ambient temperature on the travel range of electric vehicles. *IEEE Transactions on Vehicular Technology*, 65(6):4016–4022, June 2016. ISSN 0018-9545. doi:10.1109/TVT.2016.2544178.

Haijun Ruan, Jiuchun Jiang, Bingxiang Sun, Ningning Wu, Wei Shi, and Yanru Zhang. Stepwise segmented charging technique for lithium-ion battery to induce thermal management by low-temperature internal heating. In *Transportation Electrification Asia-Pacific (ITEC Asia-Pacific), 2014 IEEE Conference and Expo*, pages 1–6. IEEE, 2014.

XH Rui, Y Jin, XY Feng, LC Zhang, and CH Chen. A comparative study on the low-temperature performance of lifepo 4/c and li 3 v 2 (po 4) 3/c cathodes for lithium-ion batteries. *Journal of Power Sources*, 196(4):2109–2114, 2011.

Samveg Saxena, Caroline Le Floch, Jason MacDonald, and Scott Moura. Quantifying ev battery end-of-life through analysis of travel needs with vehicle powertrain models. *Journal of Power Sources*, 282:265–276, 2015.

Gerrit Suck and Carsten Spengler. Solutions for the thermal management of electrically driven vehicles. *ATZ worldwide*, 116(7-8):4–9, 2014.

Yashraj Tripathy, Andrew McGordon, and Chee Low. A new consideration for validating battery performance at low ambient temperatures. *Energies*, 11(9):2439, 2018.

SS Zhang, K Xu, and TR Jow. The low temperature performance of li-ion batteries. *Journal of Power Sources*, 115(1):137–140, 2003.

Fangdan Zheng, Jiuchun Jiang, Bingxiang Sun, Weige Zhang, and Michael Pecht. Temperature dependent power capability estimation of lithium-ion batteries for hybrid electric vehicles. *Energy*, 113:64–75, 2016.

DOI 10.3384/ecp19157107